

# Wilson Fermions at Finite Density as a Band Theory

J. L. Alonso<sup>1\*</sup>, L. A. Fernández<sup>1†</sup>, and V. Martín-Mayor<sup>2‡</sup>

<sup>1</sup> Departamento de Física Teórica, Universidad de Zaragoza. 50009 Spain.

<sup>2</sup> Departamento de Física Teórica I, Universidad Complutense de Madrid. 28040 Spain.

February 5, 2020

## Abstract

We analyze the feasibility of using Wilson fermions at finite density to study the physics of conduction electrons in band theory. We only include the interaction of the fermions with an external electromagnetic field. We study properties such as the density of states or the electric conductivity, both by analytical means and with numerical methods based on a path-integral formalism, finding a nice agreement. The numerical methods are generalizable to systems with dynamical interactions.

PACS numbers: 71.20.-b, 71.10.Fd, 11.15.Ha

## 1 Introduction

The study of interacting lattice fermions models has always been a difficult task in condensed-matter physics, especially from the numerical side. However, the theoretical investigations of some of the most challenging open problems in the field, like high-temperature superconductivity [1] or Colossal Magnetoresistance [2], are usually formulated in terms of lattice fermions models as the Hubbard model [3] and double-exchange models [4]. The great computational difficulties encountered in the study of these models, the so-called sign problem, can be traced back to their use of the Hamiltonian formalism of many-body systems. This has suggested the use of simpler models for the study of high-temperature superconductivity [5], formulated in the Lagrangian formalism and inspired by Wilson's field-theory on the lattice [6]. The Lagrangian lattice formalism has been widely studied in the last twenty five years in the context of Quantum Electrodynamics and Quantum Chromodynamics[7]. As a consequence powerful and sound Monte Carlo methods have been designed. Furthermore, there has been some successful investigations of lattice field-theoretical models of interacting fermions at finite density and zero temperature[8], although this is still an important technical problem[9]. In these cases, the numerical simulations are definitively easier than in a Hubbard model study, which suggest that changing the formalism can be of great benefit, if applicable.

Motivated by the above considerations, in this paper we will study the feasibility of using a model of Wilson fermions[10] at finite density coupled to an *external* electromagnetic field, to study the physics of conduction electrons in band theory. This is a well known model in lattice-gauge theory[11], where the space-time lattice is a cut-off that has to be removed. In our case, the lattice in the spatial directions is rather welcome, but the discretization of time is just a computational device, that we will see how to get rid of. In spite of its simplicity, we will show that our *free* system has an interesting band structure. It thus appear that the most natural application of the model is in condensed-matter problems, rather than in high-energy physics, where a delicate procedure of extrapolation to the *space-time continuum limit* is required.

Although the model is well known in particle physics, in condensed-matter emphasis is put on different observables. We thus have considered quantities that are never looked at in particle-physics simulations[8].

---

\*Electronic address: buj@gteorico.unizar.es

†Electronic address: laf@lattice.fis.ucm.es

‡Electronic address: victor@lattice.fis.ucm.es

In particular, we describe how can the *density of states* be measured in this formalism. For the electrical conductivity, we study the residue of the zero-frequency pole, which is purely imaginary. Since a non-vanishing value for this residue unambiguously signals a conducting phase, this is a rather interesting quantity in our opinion. To measure it, we follow a very elegant procedure due to Kohn[12]. He showed that this residue can be measured by studying the sensitivity of the ground-state energy to an external Aharonov-Bohm electromagnetic field. We show how can this be obtained in our Euclidean-time, path-integral formalism by explicitly performing the functional integrals in momentum space. However, we project to use our formalism to study more challenging interacting problems. As the Kohn procedure crucially depends on the calculation of the free-energy, it is not well suited for a Monte Carlo study of a self-interacting problem. This is why we present a different technique that can be straightforwardly generalized to interacting problems. We study the response of our system to an external electric field, that can very naturally fitted in our formulation. This technique requires a numerical calculation even in our simple model, and it is very useful as testing ground. The delicate point, however, is that our electric fields varies in *Euclidean* time. One can nevertheless assume that there is a linear relation between the Euclidean current and the Euclidean electric field, at least for small fields. This *Euclidean conductivity* presents a pole, whose residue is numerically shown to be compatible to the one obtained with the Kohn's method. Although at present we lack a rigorous proof of the equivalence of both calculations, this result gives a strong support to the linear response method.

The paper is planned as follows. In section 2 we introduce the formalism and notation. In section 3 we discuss the exact solution for free fermions in an infinite lattice, showing the band structure. In section 4 we apply the Kohn's method to obtain the residue of the conductivity pole at vanishing frequency. In section 5 we discuss how the results obtained in a four dimensional lattice can be extrapolated to continuum time. The numerical computations are presented in section 6. In subsection 6.1 we describe the results for the density of states. Subsection 6.2 is devoted to the calculation of the conductivity analyzing the linear response to a small external electric field. Our conclusions are drawn in section 7.

## 2 The Model

### 2.1 Hamiltonian Formalism

Wilson Fermions can be introduced by means of the following tight-binding Hamiltonian, in a three dimensional cubic lattice of spacing  $a_s$  [11]:

$$\begin{aligned} H = & \sum_{\xi, \eta} \sum_{\mathbf{x}} [(m_D c_F^2 + 3r_s \frac{\hbar c_F}{a_s}) d_{\mathbf{x}, \xi}^\dagger \beta_{\xi, \eta} d_{\mathbf{x}, \eta} \\ & - \frac{i}{2} \frac{\hbar c_F}{a_s} \sum_{j=1}^3 d_{\mathbf{x}, \xi}^\dagger \alpha_{\xi, \eta}^j (d_{\mathbf{x}+\hat{\mathbf{j}}, \eta} - d_{\mathbf{x}-\hat{\mathbf{j}}, \eta}) \\ & - \frac{r_s \hbar c_F}{2} \frac{\hbar c_F}{a_s} \sum_{j=1}^3 d_{\mathbf{x}, \xi}^\dagger \beta_{\xi, \eta} (d_{\mathbf{x}+\hat{\mathbf{j}}, \eta} + d_{\mathbf{x}-\hat{\mathbf{j}}, \eta})], \end{aligned} \quad (1)$$

where  $\hat{\mathbf{j}}$  is an unitary vector in the  $j$  direction,  $\xi, \eta = 1, 2, 3, 4$  are Dirac indices and

$$\beta = \gamma_0, \quad \alpha^j = i\gamma_0\gamma_j. \quad (2)$$

We shall use the following representation for the (Euclidean) gamma matrices

$$\gamma_0 = \begin{pmatrix} 0 & 1 \\ 1 & 0 \end{pmatrix}, \quad \gamma_i = \begin{pmatrix} 0 & -i\sigma_i \\ i\sigma_i & 0 \end{pmatrix}, \quad (3)$$

where  $\sigma_i$  are the Pauli matrices. The operators  $d, d^\dagger$  verify the usual anticommutation rules

$$\{d_{\mathbf{x}, \xi}, d_{\mathbf{y}, \eta}\} = \{d_{\mathbf{x}, \xi}^\dagger, d_{\mathbf{y}, \eta}^\dagger\} = 0, \quad \{d_{\mathbf{x}, \xi}^\dagger, d_{\mathbf{y}, \eta}\} = \delta_{\mathbf{x}, \mathbf{y}} \delta_{\xi, \eta}. \quad (4)$$

The diagonalization of the above Hamiltonian (see below) shows that it describes a system of four bands. The parameter  $m_D$  is intended to be of the order of the electron mass, and we will see that controls

the separation between the two upper bands from the two lower ones. The other free parameter with dimensions,  $\hbar c_F/a_s$ , will determine the band-width (it is the analogue of the  $t$  parameter in the Hubbard model), or, conversely, from the latter the velocity  $c_F$  can be obtained. The diagonalization of the Hamiltonian (1) is easier in Fourier space, where we will denote by  $e_{\mathbf{k},\xi}$  the Fourier transform of  $d_{\mathbf{x},\xi}$  and so on. Taking  $\mathbf{k}$  in units of the inverse lattice spacing, the Hamiltonian reads

$$H = \frac{\hbar c_F}{a_s} \sum_{\mathbf{k}} e_{\mathbf{k},\xi}^\dagger \Gamma_{\xi,\eta}(\mathbf{k}) e_{\mathbf{k},\eta}, \quad (5)$$

where the self-adjoint matrix  $\Gamma$  is

$$\Gamma(\mathbf{k}) = \Sigma(\mathbf{k})\gamma_0 + i \sum_j \gamma_0 \gamma_j \sin k_j, \quad (6)$$

$$\Sigma(\mathbf{k}) = m + r_s \sum_j (1 - \cos k_j), \quad (7)$$

and we have introduced the dimensionless mass as

$$m = \frac{m_D c_F}{\hbar} a_s. \quad (8)$$

The final step is the diagonalization of the  $4 \times 4$  matrix  $\Gamma(\mathbf{k})$ , from what one can finally obtain

$$H = \frac{\hbar c_F}{a_s} \sqrt{\Sigma^2(\mathbf{k}) + \Xi(\mathbf{k})} (f_{\mathbf{k},1}^\dagger f_{\mathbf{k},1} + f_{\mathbf{k},2}^\dagger f_{\mathbf{k},2} - f_{\mathbf{k},3}^\dagger f_{\mathbf{k},3} - f_{\mathbf{k},4}^\dagger f_{\mathbf{k},4}), \quad (9)$$

$$\Xi(\mathbf{k}) = \sum_j \sin^2 k_j, \quad (10)$$

where the  $f$  operators satisfy

$$\{f_{\mathbf{k},\xi}, f_{\mathbf{k}',\eta}\} = \{f_{\mathbf{k},\xi}^\dagger, f_{\mathbf{k}',\eta}^\dagger\} = 0, \quad \{f_{\mathbf{k},\xi}^\dagger, f_{\mathbf{k}',\eta}\} = \delta_{\mathbf{k},\mathbf{k}'} \delta_{\xi,\eta}. \quad (11)$$

Therefore, the system truly consists of two bands, each of them twofold degenerate (which is usually assumed to represent the electron spin), with an energy separation  $2m\hbar c_F/a_s$ . In a typical case, one may choose  $r_s = 1$ , and the width of the upper band would be  $6\hbar c_F/a_s$ , independently of  $m$ . Therefore, if one is interested in a problem for which the interband transitions can be safely disregarded, the value of  $m$  should be made rather large while the chemical potential is to be placed within the upper band (actually, it could equivalently be placed within the lower one). The density of states for the upper band is represented in figure 1. Notice that for large  $m$ , the dispersion relation in Eq. (9), up to terms of order  $1/m$ , is equal to

$$E(\mathbf{k}) = \frac{\hbar c_F}{a_s} [m + r_s \sum_j (1 - \cos k_j)], \quad (12)$$

and we recover the usual hopping term of the cubic lattice, with its well known particle-hole symmetry. Let us finally mention that the Hamiltonian (1) has been extensively used for the non-perturbative study of high-energy physics. These studies require a delicate extrapolation procedure known as *taking the continuum limit* (see for instance Ref. [11]), in which one recovers the relativistic symmetry when taking  $c_F = c$ . Fortunately there is no need of this extrapolation in the Condensed Matter applications that we are envisaging. Therefore  $c_F$  is a parameter that can be tuned in order to obtain the band width appropriated to the specific physical system of interest. In fact, if we consider a lattice spacing  $a_s \sim 1\text{\AA}$ , and typical energies  $\hbar c_F/a_s \sim 10\text{ eV}$ , one obtains  $c_F \sim 0.005c$  which is about the Fermi speed of an usual conductor. With this selection of  $c_F$ , we have for the dimensionless mass  $m \sim 1$  when  $m_D$  is of the order of the electron mass.

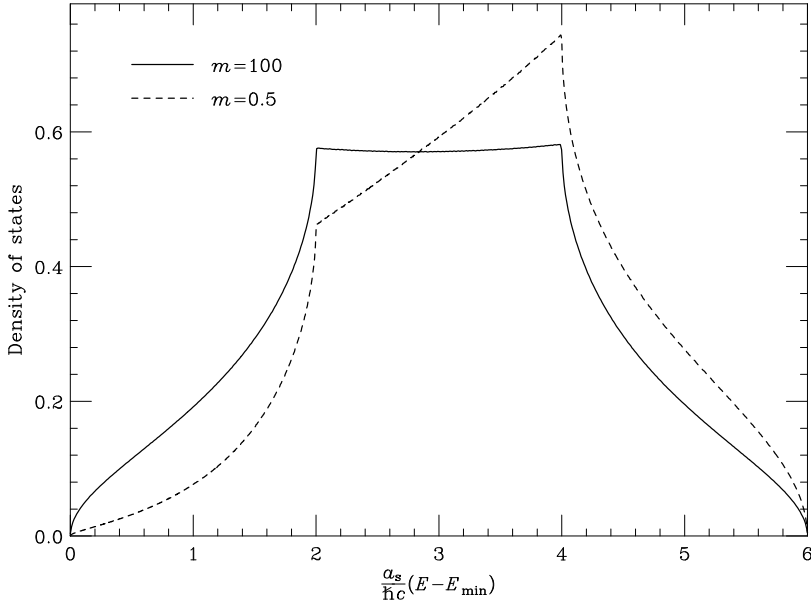


Figure 1: The density of states of the upper band of the Hamiltonian (1), with  $r_s = 1$  and  $m = 0.5, 100$ , as a function of the energy measured from the band-minimum.

## 2.2 Lagrangian Formalism

The Lagrangian formulation appears naturally when calculating the partition function of the system defined in Eq. (1) in the path-integral formalism (see for example Ref. [13]). In order to be able of performing the path integral numerically we shall discretize the time with a spacing  $a_t$ . Of course, this is only an artifact that must be removed by a proper continuum-time limit extrapolation (see section 5). It will be convenient to consider our massive Wilson fermions coupled to an *external* electromagnetic field.

In the following we will choose units such that  $k_B = 1$ ,  $\hbar = 1$ , and  $c_F = 1$ . Therefore energies are measured in units of  $1/a_t$  and momenta in units of  $1/a_s$ . However, the partition function should be written in terms of dimensionless quantities. For instance, the chemical potential entering in the partition function,  $\mu$ , will be the physical dimensionful one,  $\mu_D$ , times  $a_t$ , and the mass  $m$ , will be  $m_D a_s$ .

Our starting partition function (Euclidean time) can be written as (the  $*$  superscript stands for complex conjugation) [14, 15, 16]

$$\mathcal{Z}[U] = \int \prod_z d\Psi_z d\bar{\Psi}_z \exp \left[ \sum_{x,y} \bar{\Psi}_x M_{xy}(U) \Psi_y \right]. \quad (13)$$

$$\begin{aligned} M_{xy}(U) &= e^{\lambda\mu} U_{x,0}(\gamma_0 - r_t) \delta_{y,x+\hat{\nu}} - e^{-\lambda\mu} U_{x,0}^*(\gamma_0 + r_t) \delta_{y+\hat{\nu},x} \\ &+ \lambda \sum_{i=1}^3 [U_{x,i}(\gamma_i - r_s) \delta_{y,x+\hat{i}} - U_{x,i}^*(\gamma_i + r_s) \delta_{y+\hat{i},x}] + [(2m + 6r_s)\lambda + 2r_t] \delta_{x,y}, \end{aligned} \quad (14)$$

where  $U_{x,\nu} = e^{iA_{x,\nu}}$ ,  $A$  being the gauge field, and  $\Psi_x$ ,  $\bar{\Psi}_x$  are the anticommuting Grassmann fermionic fields. Here,  $x, y$  run on the points of the four-dimensional space-time lattice. We impose periodic boundary conditions for the gauge field, and periodic in space but antiperiodic in time ( $\nu = 0$ ) for the Grassmann field. The site  $x + \hat{\nu}$  is the neighbor of  $x$  in the  $\nu = 0, 1, 2, 3$  direction. For finite temporal length,  $L_0$ , the system is at finite temperature  $T = (a_t L_0)^{-1}$ . In this paper we will only consider the zero temperature ( $L_0 \rightarrow \infty$ ) limit. We follow the prescription of introducing the chemical potential through an imaginary gauge field  $A = (-i\lambda\mu, 0, 0, 0)$  [14, 15], which is fairly convenient for analytical calculations. The parameter  $\lambda$  can be formally identified with  $a_t/a_s$  in the classical action. For now, let us just say

that the formal time continuum limit is obtained when  $\lambda \rightarrow 0$ , and that in this limit  $\lambda$  can be consistently identified with  $a_t/a_s$  (see section 5). In this limit, one has  $e^{\lambda\mu} \approx 1 + \lambda\mu$ , and as the interesting values of the chemical potential  $\mu$  can be rather large (see Fig. 1), it will prove convenient to define

$$e^{\lambda\mu} = 1 + \lambda\mu'. \quad (15)$$

Although in the temporal continuum limit,  $\lambda \rightarrow 0$ ,  $\mu$  tends to  $\mu'$ , we shall show in section 5 that the convergence of the interesting quantities is much faster in terms of  $\mu'$ .

The Gaussian path-integral in Eq. (13) and the associate propagators, can be formally solved as

$$\mathcal{Z}[U] = \det M(U), \quad \langle \Psi_x \bar{\Psi}_y \rangle = M_{xy}^{-1}. \quad (16)$$

To define the electric four-current in the lattice, we recall that (formally) in the space-time continuum limit we can write the partition function as

$$\mathcal{Z}[A] = \int D\Psi D\bar{\Psi} \exp \left[ \int d^4x \bar{\Psi} \gamma_\nu (\partial_\nu - ie A_\nu) \Psi + m \bar{\Psi} \Psi \right]. \quad (17)$$

Taking functional derivatives, we obtain

$$\frac{\delta \log \mathcal{Z}}{\delta A_\nu(x)} = \langle j_\nu(x) \rangle, \quad (18)$$

where

$$j_\nu(x) = \bar{\Psi}(x) \gamma_\nu \Psi(x). \quad (19)$$

This calculation can be exactly mimicked on the lattice, if we notice that a change in the link variable should be of the form  $U_{x,\nu} \rightarrow e^{i\alpha_{x,\nu}} U_{x,\nu}$ . In this way we obtain [15]:

$$\langle j_{x,\nu} \rangle = i \frac{\partial \log \mathcal{Z}}{\partial \alpha_{x,\nu}}, \quad (20)$$

where now

$$\langle j_{x,0} \rangle = \langle \bar{\Psi}_x e^{\lambda\mu} U_{x,0} (\gamma_0 - r_t) \Psi_{x+\hat{0}} + \bar{\Psi}_{x+\hat{0}} e^{-\lambda\mu} U_{x,0}^* (\gamma_0 + r_t) \Psi_x \rangle \quad (21)$$

$$\langle j_{x,i} \rangle = \lambda \langle \bar{\Psi}_x U_{x,i} (\gamma_i - r_s) \Psi_{x+i} + \bar{\Psi}_{x+i} U_{x,i}^* (\gamma_i + r_s) \Psi_x \rangle, \quad i = 1, 2, 3. \quad (22)$$

The  $j_0$  component is just the electric charge density that one encounters by differentiating with respect to  $\lambda\mu$  the Free Energy density [15]. Moreover, from the gauge invariance of the determinant of the fermionic matrix,  $M$ , it is straightforward to prove the lattice continuity equation, for any configuration of the electromagnetic-field (actually, this is a nice program's check):

$$0 = \sum_\nu (\langle j_{x,\nu} \rangle - \langle j_{x-\hat{\nu},\nu} \rangle). \quad (23)$$

Eqs. (21) and (22) can be written free of Grassmann variables as

$$-\langle j_{x,0} \rangle = e^{\lambda\mu} U_{x,0} \text{Tr}[(\gamma_0 - r_t) M_{x+\hat{0},x}^{-1}] + e^{-\lambda\mu} U_{x,0}^* \text{Tr}[(\gamma_0 + r_t) M_{x,x+\hat{0}}^{-1}], \quad (24)$$

$$-\langle j_{x,i} \rangle = \lambda U_{x,i} \text{Tr}[(\gamma_i - r_s) M_{x+i,x}^{-1}] + \lambda U_{x,i}^* \text{Tr}[(\gamma_i + r_s) M_{x,x+i}^{-1}], \quad (25)$$

where  $\text{Tr}$  stands for the trace over Dirac indices. The above expressions and the relations

$$\gamma_\nu^* = \gamma_1 \gamma_3 \gamma_\nu \gamma_3 \gamma_1, \quad (26)$$

$$M(U^*) = \gamma_1 \gamma_3 (M(U))^* \gamma_3 \gamma_1, \quad (27)$$

$$M^{-1}(U^*) = \gamma_1 \gamma_3 (M^{-1}(U))^* \gamma_3 \gamma_1, \quad (28)$$

allow to prove that

$$\langle j_{x,\nu} \rangle_U^* = \langle j_{x,\nu} \rangle_{U^*}. \quad (29)$$

In an uniform electrical field, the charge density should remain constant under field inversion, while the electrical current should change sign. Therefore, from Eq. (29) one expects the former to be real and the latter to be imaginary (Euclidean space-time!).

### 3 The Band Structure

In absence of external fields ( $U = 1$ ) the matrix  $M$  can be diagonalized in Fourier space, which allows to explicitly perform the functional integrals, and to compute the Free Energy or the propagator. Even in this free case, the results present a very interesting structure.

We will consider a lattice of volume  $V = L_0 \times L_1 \times L_2 \times L_3$ ,  $L_\nu$  being the number of sites in the  $\nu$  direction, with periodic boundary conditions in the spatial directions and antiperiodic in the time one. Let us define the discrete Fourier transform of the fermion field as

$$\hat{\Psi}_k = \frac{1}{\sqrt{V}} \sum_x e^{-ik \cdot x} \Psi_x, \quad k_i = \frac{2\pi}{L_i} n_i, \quad k_0 = \frac{2\pi}{L_i} \left( n_0 + \frac{1}{2} \right). \quad (30)$$

The components of  $x$  are integers in the range  $[0, L_\nu - 1]$ , as well as the  $n_\nu$ .

The transform for the fermionic matrix is thus

$$\hat{M}_{k'k} = \frac{1}{V} \sum_{x,y} e^{-ik' \cdot x + ik \cdot y} M_{xy} = 2\delta_{k'k} \Delta_k, \quad (31)$$

where  $\Delta_k$  is the  $4 \times 4$  matrix

$$\Delta_k = \lambda \left( \Sigma(\mathbf{k}) + i \sum_i \gamma_i \sin k_i \right) + 2r_t \sin^2 \frac{k_0 - i\lambda\mu}{2} + i\gamma_0 \sin(k_0 - i\lambda\mu). \quad (32)$$

Using the properties of  $\gamma$  matrices and the definitions in Eqs. (7) and (10), the inverse propagator reads

$$\Delta_k^{-1} = \frac{\lambda \Sigma(\mathbf{k}) - i\lambda \sum_i \gamma_i \sin k_i - i\gamma_0 \sin(k_0 - i\lambda\mu)}{[\lambda \Sigma(\mathbf{k}) + 2r_t \sin^2 \frac{k_0 - i\lambda\mu}{2}]^2 + \lambda^2 \Xi(\mathbf{k}) + \sin^2(k_0 - i\lambda\mu)}. \quad (33)$$

We can also calculate the free energy density,  $f_D = a_s^{-3} a_t^{-1} f$ . Let us call  $V_{s,D}$  to the spatial lattice volume. We obtain

$$f_D = -\frac{T}{V_{s,D}} \log \mathcal{Z} = -\frac{1}{L_0 a_t} \frac{1}{L_1 L_2 L_3 a_s^3} \log \mathcal{Z}, \quad (34)$$

$$f = -\frac{1}{V} \sum_k \log \det \Delta_k, \quad (35)$$

$$= -\frac{2}{V} \sum_k \log \left[ \left( \lambda \Sigma(\mathbf{k}) + 2r_t \sin^2 \frac{k_0 - i\lambda\mu}{2} \right)^2 + \lambda^2 \Xi(\mathbf{k}) + \sin^2(k_0 - i\lambda\mu) \right]. \quad (36)$$

Notice that the physically interesting quantity is obtained after subtracting the vacuum contribution, that is

$$\tilde{f}(\mu) = f(\mu) - f(0). \quad (37)$$

With the previous results at hand we can compute all quantities of interest. For example, the charge density,  $\langle j_{x,0} \rangle$ , which is site independent, can be written as

$$\rho(\lambda, \mu) \equiv \langle j_{x,0} \rangle = -\frac{\partial \tilde{f}}{\lambda \partial \mu} \quad (38)$$

$$= -\frac{4i}{V} \sum_k \frac{\sin(k_0 - i\lambda\mu) \{ \cos(k_0 - i\lambda\mu) + r_t [\lambda \Sigma(\mathbf{k}) + 2r_t \sin^2 \frac{k_0 - i\lambda\mu}{2}] \}}{[\lambda \Sigma(\mathbf{k}) + 2r_t \sin^2 \frac{k_0 - i\lambda\mu}{2}]^2 + \lambda^2 \Xi(\mathbf{k}) + \sin^2(k_0 - i\lambda\mu)}. \quad (39)$$

Notice that at  $\mu = 0$  the summand is odd in  $k_0$  and the net charge density is zero as it should. In the  $L_0 \rightarrow \infty$  limit (zero temperature) the  $k_0$  sum becomes an integral that can be performed by the residue method. We consider the rectangle in the  $k_0$  plane with vertices at  $(\pi, 0)$ ,  $(\pi, i\lambda\mu)$ ,  $(-\pi, i\lambda\mu)$ ,  $(-\pi, 0)$ . The integrals along the two vertical segments cancel out by periodicity, and that along the upper horizontal side vanishes by parity. Therefore, the integral along the real segment is equal to that over the

closed path (see Refs. [11, 17] for similar calculations). The integrand has poles of residue 1/2 (notice that the numerator in Eq. (39) is one half of the derivative of the denominator) at

$$k_0 = 2n\pi + i(\lambda\mu \pm E_1(\mathbf{k})), \quad (40)$$

$$k_0 = (2n+1)\pi + i(\lambda\mu \pm E_2(\mathbf{k})), \quad (41)$$

where

$$E_{1,2}(\mathbf{k}) = \operatorname{arccosh} \left[ \frac{\sqrt{(1+\lambda^2\Xi(\mathbf{k}))(1-r_t^2) + (\lambda\Sigma(\mathbf{k})+r_t)^2} \mp r_t(\lambda\Sigma(\mathbf{k})+r_t)}{1-r_t^2} \right]. \quad (42)$$

If we approach the singular value  $r_t = 1$  from below  $E_2(\mathbf{k})$  diverges, while  $E_1(\mathbf{k})$  tends to

$$E_1^{(r_t=1)}(\mathbf{k}) = \operatorname{arccosh} \left[ \frac{1+\lambda^2\Xi(\mathbf{k}) + (\lambda\Sigma(\mathbf{k})+1)^2}{2(\lambda\Sigma(\mathbf{k})+1)} \right]. \quad (43)$$

In the infinite volume limit one gets ( $\mu > 0$ )

$$\rho(\lambda, \mu) = 2 \int_{-\pi}^{\pi} \frac{d^3 k}{(2\pi)^3} [\theta(\mu - \lambda^{-1}E_1(\mathbf{k})) + \theta(\mu - \lambda^{-1}E_2(\mathbf{k}))]. \quad (44)$$

A very useful quantity is

$$\kappa(\lambda, \mu) = \frac{\partial \rho(\lambda, \mu)}{\partial \mu}, \quad (45)$$

that can be related with the compressibility by

$$-\frac{1}{V_s} \frac{\partial V_s}{\partial P} \Big|_{T,N} = \frac{1}{\rho^2} \kappa. \quad (46)$$

From Eq.(44) we obtain

$$\kappa(\lambda, \mu) = 2 \int_{-\pi}^{\pi} \frac{d^3 k}{(2\pi)^3} [\delta(\mu - \lambda^{-1}E_1(\mathbf{k})) + \delta(\mu - \lambda^{-1}E_2(\mathbf{k}))], \quad (47)$$

$$= 2\lambda \int_{E_1(\mathbf{k})=\lambda\mu} \frac{d^2 S}{(2\pi)^3} \frac{1}{\|\nabla_{\mathbf{k}} E_1(\mathbf{k})\|} + 2\lambda \int_{E_2(\mathbf{k})=\lambda\mu} \frac{d^2 S}{(2\pi)^3} \frac{1}{\|\nabla_{\mathbf{k}} E_2(\mathbf{k})\|}. \quad (48)$$

The last expression strongly reminds the definition of the *density of states* of a Fermi system [18], and  $\kappa(\lambda, \mu)$  will be called with this name in the following. Nevertheless, the equivalence between  $\kappa$  and the density of states would not be exact at non-zero temperature. Thus, at finite time-lattice spacing, the system can be thought of as being composed by four bands of energies  $\pm E_1(\mathbf{k})$ ,  $\pm E_2(\mathbf{k})$  (notice that the normalization of two electrons per site and band is rather natural). The Dirac sea is rather a Fermi sea, where at zero chemical potential the two lower bands are full, but the upper ones are empty and the density of states is zero at Fermi level. When the chemical potential reaches a band minimum, the particle band starts to fill until the maximum is reached. We will show that further rising of the chemical potential has no physical effect since the density of states drop to zero again and the fermion system gets rather insensitive to external perturbations. One would expect a similar insensitivity at zero chemical potential, but it should be kept in mind that it is always possible to move an electron from the filled to the empty bands.

Regarding the  $r_t$  dependence of the energies, we see that for  $r_t = 0$  the two bands are degenerated. If we approach the singular value  $r_t = 1$  from below, the only finite energy band is the associated to  $E_1(\mathbf{k})$ . In the intermediate case, there will be two different bands whose overlapping depend on  $r_t$ . The value of  $r_s$  affects to the shape of the dispersion relation. For  $r_s = 0$  the lower band limit is at  $\mathbf{k} = (n_1\pi, n_2\pi, n_3\pi)$ , the  $n$ 's being integers, while for  $r_s > 0$  there is only one absolute minimum in each Brillouin zone.

The band structure of the numerical examples that we will consider in this work ( $\lambda = 1$ ,  $m = 1/2$ ,  $r_s = r_t = 0, 0.5, 1$ ) is shown in Fig. 2, while the density of states is shown in Fig. 3. In all the figures of

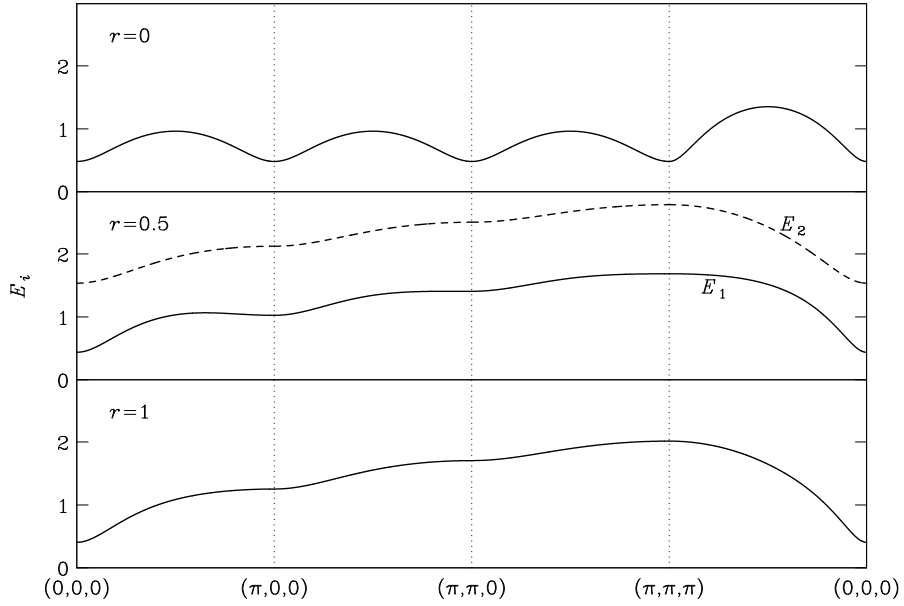


Figure 2: Energy bands  $E_1$ ,  $E_2$  along symmetry lines of the cubic reciprocal lattice for  $m = 1/2$ ,  $\lambda = 1$ , and  $r = r_s = r_t = 0, 0.5, 1$

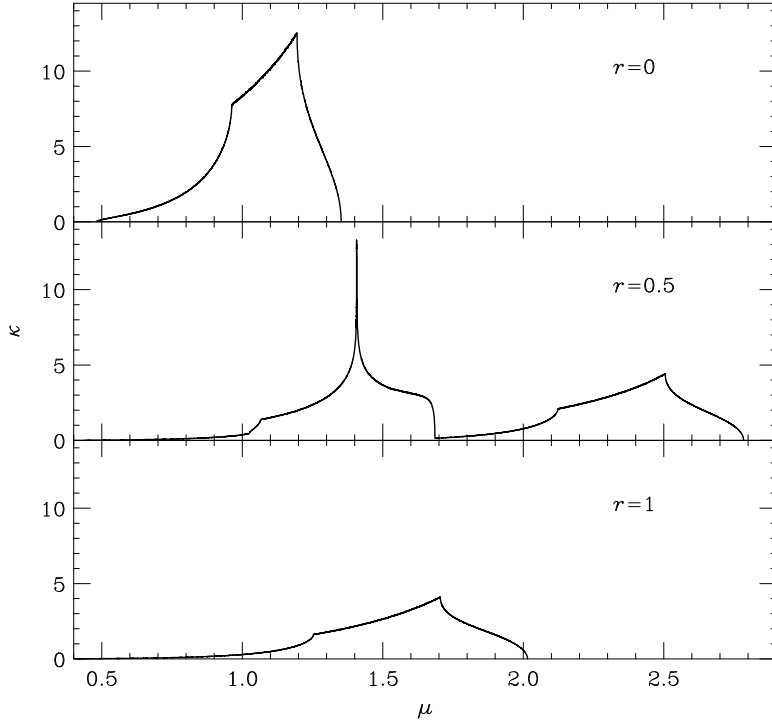


Figure 3: The density of states for  $m = 1/2$  with several values of the Wilson parameter  $r$ .

in this paper we have taken  $r = r_s = r_t$ . The rationale for choosing such a small  $m$ , is that we want to test the feasibility of the numerical calculations in a rather demanding situation.

The energies been measured in units of  $a_t^{-1}$ , if they are to remain finite in the temporal continuum

limit, they should tend to zero as  $\lambda$ . Notice that in this limit, for  $r_t > 0$ , we have

$$E_1(\mathbf{k}) = \lambda \sqrt{\Sigma^2(\mathbf{k}) + \Xi(\mathbf{k})} + O(\lambda^2), \quad (49)$$

while  $E_2(\mathbf{k})$  do not approach zero. Consequently, it is divergent in physical units, while  $E_1(\mathbf{k})$  tends to the value in Eq. (9), and we recover the target theory.

## 4 The Electrical Conductivity

In a classical paper, Kohn [12] developed an elegant characterization of a conductor, at zero temperature. His method allows the measurement of the following limit for the imaginary part of the electrical conductivity,  $\sigma''_D$ ,

$$Z_D = \lim_{\omega_D \rightarrow 0} \omega_D \sigma''_D(\omega_D). \quad (50)$$

If this limit turns out to be non zero, the system is a conductor. The construction was as follows. The system of interest is constrained to verify periodic boundary conditions in the (say) first spatial direction, and immersed in a Aharonov-Bohm like electromagnetic field  $A_D = (0, \alpha_D, 0, 0)$ . With this choice of boundary conditions the product  $L_1 a_s \alpha_D$  is gauge invariant since it represents the magnetic flux traversing the system. Kohn was able to show that

$$Z_D = -\frac{1}{V_{s,D}} \left. \frac{d^2 E_{0,D}}{d\alpha_D^2} \right|_{\alpha_D=0}, \quad (51)$$

where  $E_{0,D}$  is the ground-state energy. It is crucial that the infinite limit volume is taken *after* the  $\alpha$  derivative is performed, since the effect of the Aharonov-Bohm field can be thought of as a change in the boundary conditions (see below). In the infinite volume limit, the energy no longer depends on  $\alpha_D$ .

In our case, as the free energy and the internal energy coincide in the zero temperature limit, we can study the residue in the following way

$$Z = -\lim_{V_s \rightarrow \infty} \lim_{T \rightarrow 0} \left. \frac{d^2 \tilde{f}}{d\alpha^2} \right|_{\alpha=0}, \quad (52)$$

where we have use only dimensionless quantities.

The free energy can be calculated in a finite volume and at finite temperature as in Eq. (36). Now let us introduce our system in the Aharonov-Bohm electromagnetic field:

$$U_{x,0} = U_{x,2} = U_{x,3} = 1, \quad U_{x,1} = e^{i\alpha}. \quad (53)$$

This field can be transformed into a boundary effect by performing the following gauge transformation:

$$U_{x,\nu} \rightarrow U_{x,\nu}^G = e^{ig(x)} U_{x,\nu} e^{-ig(x+\hat{\nu})}, \quad g(x) = \alpha x_1, \quad (54)$$

so that  $U^G = 1$  excepting

$$U_{(x_1=L_1-1),1}^G = e^{i\alpha L_1}. \quad (55)$$

By direct inspection of the fermion matrix in Eq. (14), one can easily recognize that a system verifying periodic boundary conditions in the 1 direction in the field  $U^G$  is equivalent the same system with no field at all, but verifying

$$\Psi(x_0, x_1 + L_1, x_2, x_3) = e^{i\alpha L_1} \Psi(x_0, x_1, x_2, x_3), \quad (56)$$

This amounts to substituting  $k_1$  by  $k_1 + \alpha$  everywhere in Eq. (36). Once the  $\alpha$  derivative is performed, the zero temperature limit can be taken by transforming the  $k_0$  sum into an integral. The calculation follows the lines of the charge density in the previous section. We get from Eq. (52)

$$Z = -2 \int_{-\pi}^{\pi} \frac{d^3 \mathbf{k}}{(2\pi)^3} \left[ \frac{\partial^2 E_1(\mathbf{k})}{\partial k_1^2} \theta(\mu - \lambda^{-1} E_1(\mathbf{k})) + \frac{\partial^2 E_2(\mathbf{k})}{\partial k_1^2} \theta(\mu - \lambda^{-1} E_2(\mathbf{k})) \right], \quad (57)$$

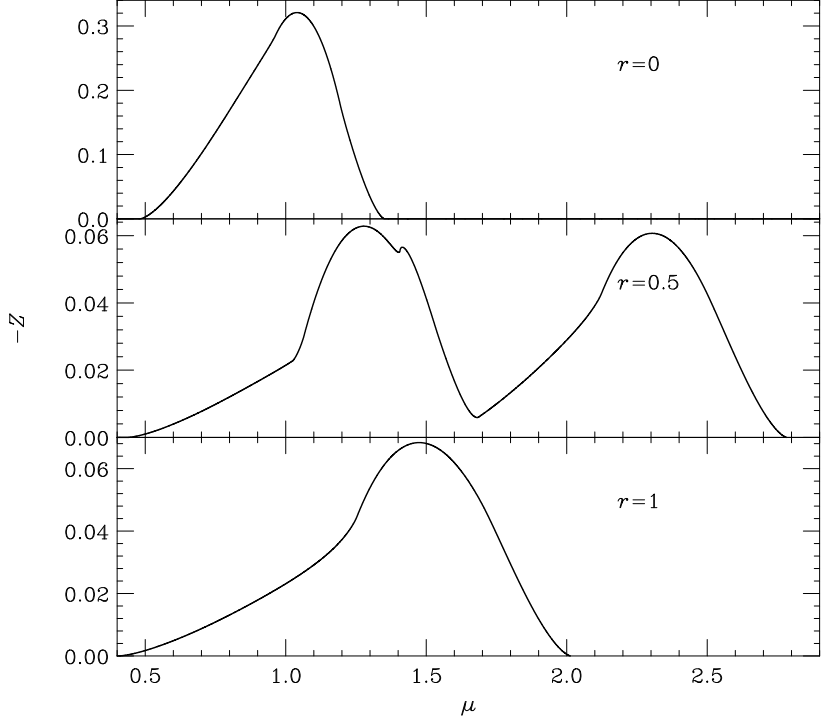


Figure 4: The limit  $\omega\sigma''(\omega)$  when  $\omega \rightarrow 0$  obtained from Eq. (57).

where we have used the property

$$\text{Res} \left[ \frac{\partial^2}{\partial \alpha^2} \log (\varphi(z; \alpha)), z_0(\alpha) \right] = -\frac{\partial^2 z_0}{\partial \alpha^2}, \quad (58)$$

$\varphi(z; \alpha)$  being an analytic function of  $z$  with a simple zero at  $z_0$ .

Notice that for the empty system ( $\mu < \lambda^{-1} \min(E_1, E_2)$ ), both integrals vanish, as well as for the full band  $\mu > \lambda^{-1} \max(E_1, E_2)$ , since  $E_{1,2}$  are periodic functions of  $k_1$ . The three dimensional integrals (57) can be performed using a Monte Carlo method. It turns out that the second derivative of the energy is simpler if calculated numerically, as the explicit expressions for the energy are involved (see Eqs. (42,43)). The results are shown in Fig. 4. Notice in particular for  $r = 0.5$  the close correspondence between the singularities of the density of states and the behavior of the conductivity residue.

In relativistic lattice-field theory calculations [17], people have calculated not only the free energy density, but also the internal energy density ( $\mathcal{E}$ ), deriving the former with respect to the temperature ( $1/T = a_t L_0$ ). This calculation strongly relies on the equivalence  $\lambda = a_t/a_s$  that for finite  $a_s$  is only appropriate in the  $\lambda \rightarrow 0$  limit. Then, one could say that

$$Z \approx - \lim_{V_s \rightarrow \infty} \lim_{T \rightarrow 0} \frac{d^2 \mathcal{E}}{d \alpha^2} \Big|_{\alpha=0}, \quad (59)$$

and get following the same type of calculation as before

$$Z = -2 \int_{\pi}^{\pi} \frac{d^3 \mathbf{k}}{(2\pi)^3} \left[ \frac{\partial^2 \mathcal{E}_1(\mathbf{k})}{\partial k_1^2} \theta(\mu - \lambda^{-1} E_1(\mathbf{k})) + \frac{\partial^2 \mathcal{E}_2(\mathbf{k})}{\partial k_1^2} \theta(\mu - \lambda^{-1} E_2(\mathbf{k})) \right], \quad (60)$$

where the functions  $\mathcal{E}_{1,2}$  are given by

$$\mathcal{E}_{1,2}(\mathbf{k}) = \frac{\lambda^2 \Sigma(\mathbf{k}) + \lambda^2 \Xi(\mathbf{k}) + r_t \lambda \Sigma(\mathbf{k}) [1 - \cosh E_{1,2}(\mathbf{k})]}{\sinh E_{1,2}(\mathbf{k}) \{ \cosh E_{1,2}(\mathbf{k}) \pm r_t [\lambda \Sigma(\mathbf{k}) + r_t (1 \mp \cosh E_{1,2}(\mathbf{k}))] \}}. \quad (61)$$

In the  $\lambda \rightarrow 0$  limit,  $\mathcal{E}_1(\mathbf{k}) \rightarrow E_1(\mathbf{k})$ . Thus, in the continuum time limit, the value of  $Z$  calculated as in Eq. (59) is the same as the one calculated with Eq. (52), but the convergence to the continuum limit is extremely slow (see next section).

## 5 Temporal continuum limit

In contrast with similar calculations in High-Energy Physics, in Condensed Matter the temporal and spatial discretization play very different roles. While the spatial one is fully physical, the temporal discretization is just a computational device that needs to be removed. In the  $a_t \rightarrow 0$  limit the only remaining quantity with dimensions is  $a_s$ . Therefore the quantities with dimensions (denoted by a D subscript) that we are after should be expressed as dimensionless quantities (denoted by a star superscript) times a power of  $a_s$ ; for instance:

$$\mu_D = a_s^{-1} \mu^*, \quad (62)$$

$$\rho_D = a_s^{-3} \rho^*, \quad (63)$$

$$Z_D = a_s^{-2} Z^*. \quad (64)$$

Pure number functions as  $\rho^*(\mu^*)$ ,  $Z^*(\mu^*)$  are the target for the continuum-time extrapolation.

On the other hand, for a finely grided discrete time (*i.e.*  $a_t \ll a_s$ ), we can consider the action in Eq. (14) as a faithful discretization of the continuum time target theory. In this limit the finite differences approach the derivative and  $\lambda$  truly represents  $a_t/a_s$ , the energies being measured in units of  $a_t^{-1}$ . We thus have:

$$\mu_D = a_t^{-1} \mu \lambda, \quad (65)$$

$$\rho_D = a_s^{-3} \rho, \quad (66)$$

$$Z_D = a_s^{-1} a_t^{-1} Z. \quad (67)$$

Since both representations Eqs. (62,63,64) and Eqs. (65,66,67) should hold true in the  $\lambda \rightarrow 0$  limit, the existence of the continuum time limit requires:

$$\mu \rightarrow \mu^*, \quad (68)$$

$$\rho(\lambda, \mu) \rightarrow \rho^*(\mu^*), \quad (69)$$

$$\lambda^{-1} Z(\lambda, \mu) \rightarrow Z^*(\mu^*). \quad (70)$$

Therefore, we obtain two consistency conditions for the existence of the continuum limit, namely that  $\rho(\lambda, \mu)$  and  $Z(\lambda, \mu)/\lambda$  are only functions of  $\mu$  for small  $\lambda$ . In our case, both for  $r_t = 0$  or  $r_t = 1$ , these conditions are fulfilled (see Eqs. (44,49,57)). For  $r_t = 0$ , we have two degenerate bands in the continuum limit while for  $r_t = 1$  there is only one. If one would be interested in a situation with two bands of similar energies, a tuning of  $r_t$  as  $r_t \sim r_t^* \lambda$  could be considered; otherwise the second band disappears.

In a more interesting problem, with interactions switched on, a possible strategy could be to produce a large number of data for different values of  $\lambda$ , and try to fit them to the previous scaling laws (69,70). However this is a painful procedure, because the smaller is  $\lambda$  the larger needs to be the temporal length of the lattice in order to get the same physical temperature. Moreover, the needed  $\lambda$  values are rather small (see below). However, we will now show that there is a very simple way of accelerating the convergence to the continuum time, by considering a non-linear transformation of  $\mu$ . For simplicity, let us restrict ourselves to  $r_s = r_t = 1$ . We consider the parameter  $\mu'$  defined in Eq. (15). Of course, when  $\lambda$  tends to zero, the differences between  $\mu$  and  $\mu'$  are immaterial. However, at finite  $\lambda$  the advantages of using  $\mu'$  are clear when considering the band limits,

$$\mu_{\min} = \lambda^{-1} \log(1 + \lambda m), \quad (71)$$

$$\mu_{\max} = \lambda^{-1} \log(1 + \lambda(m + 6)), \quad (72)$$

that become  $\lambda$  independent for  $\mu'$

$$\mu'_{\min} = m, \quad (73)$$

$$\mu'_{\max} = m + 6. \quad (74)$$

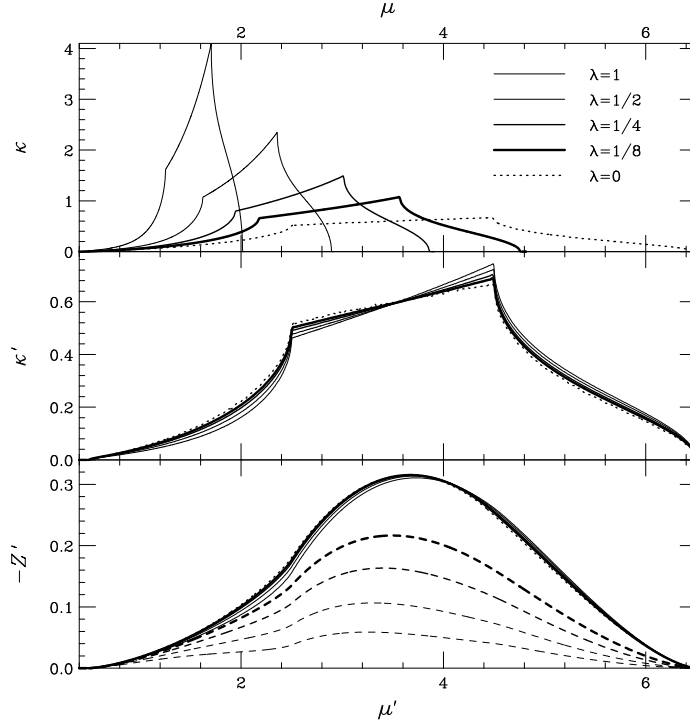


Figure 5: Temporal continuum limit for the density of states (upper and middle side) and conductivity residue (lower part). In the upper part we have used the  $\mu$  variable of Eq. (14), while in the other cases we have been used the non-linear transformation  $\mu \rightarrow \mu'$  (See Eqs. (15,76,78)). The dashed lines for the residue have been obtained using the internal energy, Eq. (59).

We can consider the following two finite- $\lambda$  approximations to the density of states:

$$\kappa^*(\mu^*) = \frac{d\rho^*(\mu^*)}{d\mu^*} \approx \frac{\partial\rho(\lambda, \mu)}{\partial\mu} = \kappa(\lambda, \mu). \quad (75)$$

and

$$\kappa^*(\mu^*) \approx \frac{\partial\mu}{\partial\mu'} \frac{\partial\rho(\lambda, \mu)}{\partial\mu} \Big|_{\mu(\mu', \lambda)} = \frac{1}{1 + \lambda\mu'} \frac{\partial\rho(\lambda, \mu)}{\partial\mu} \Big|_{\mu(\mu', \lambda)} = \kappa'(\lambda, \mu'). \quad (76)$$

We compare the performance of both extrapolations to the continuum time limit in Fig. 5. In the upper part we use Eq. (75), while in the central plot we show the results obtained with Eq. (76). We believe that the advantages of the non-linear transformation (15) need no further advertising.

For the residue of the conductivity, we follow a similar procedure. Instead of the naive approximant,

$$Z^*(\mu^*) \approx \lambda^{-1} Z(\lambda, \mu) \quad (77)$$

it is better to use

$$Z^*(\mu^*) \approx \frac{1 + \lambda\mu'}{\lambda} Z(\lambda, \mu) \Big|_{\mu(\mu', \lambda)} = Z'(\lambda, \mu') \quad (78)$$

In the lower part of Fig.(5) we show the continuum limit extrapolation obtained with Eq. (78) for several  $\lambda$  values. The performance is again rather satisfactory. In the same plot, we show the estimate of the residue obtained from the internal energy instead of the free energy (the rescaling factor is the same as in Eq. (78)). Although in the continuum-time limit (dotted line) both estimates coincide, the convergence is much faster for the free-energy.

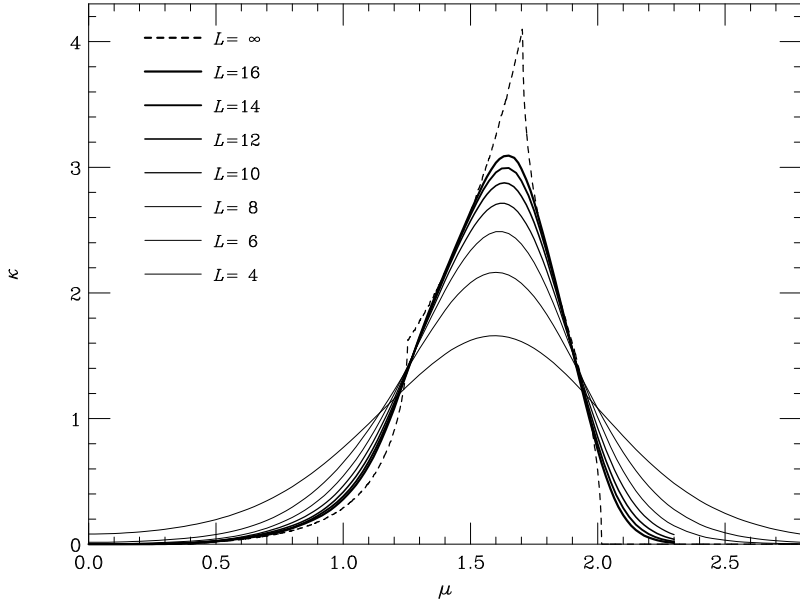


Figure 6: Density of states computed numerically, for  $r = 1, \lambda = 1$ , in finite lattices of sizes 4, 6, 8, 10, 12, 14, 16. The infinite volume limit has been obtained with the methods in Section 3.

## 6 Numerical Calculations

In this section, we are going to reproduce the results of the sections 4 and 5 by directly considering the integration of the partition function. This method has the advantage of being generalizable to inhomogeneous external fields, or even to the presence of interacting dynamical fields. To compute the partition function it is necessary to work in finite lattices, consequently, one should take the infinite volume limit at the end.

We have carried out measures in symmetric lattices of sizes  $L = 4, 6, 8, 10, 12, 14$  and  $16$ , with  $m = 1/2$  and  $\lambda = 1$ . For the hopping term, we have used  $r = r_s = r_t$ . As the integral in the fermionic fields is Gaussian, the computation of the electric current just requires the inversion of a  $4V$  matrix,  $V$  being the space-time volume. As the fermion matrix (14) is sparse, we have used a conjugate-gradient algorithm for the numerical inversion.

### 6.1 Density of States

We first consider the density of states in a vanishing external field. In order to measure  $\partial\rho/\partial\mu$  we invert the matrix at  $\mu \pm \epsilon$  for  $\epsilon$  small enough. In interacting systems the derivative can be calculated in terms of connected correlation-functions [11].

The numerical results are plotted in Figs. 6 and 7, together with the infinite volume values obtained in section 3. Although the finite size effects are non negligible even in the larger lattices for most values of  $\mu$ , there is a clear trend to the asymptotic values.

### 6.2 Linear Response

Unfortunately, for an interacting system it is not immediate how to implement Kohn's method for calculating the residue of the conductivity. In fact, the free energy is rather hard to calculate with a Monte Carlo simulation and what one directly obtains are mean-values. We are now going to present a different way of computing the residue, by directly measuring the system response to an external electrical field. Notice that the presence of an electric field requires a non-homogeneous vector potential and consequently the inversion of the fermion matrix can no longer be performed in closed analytical form. This new recipe

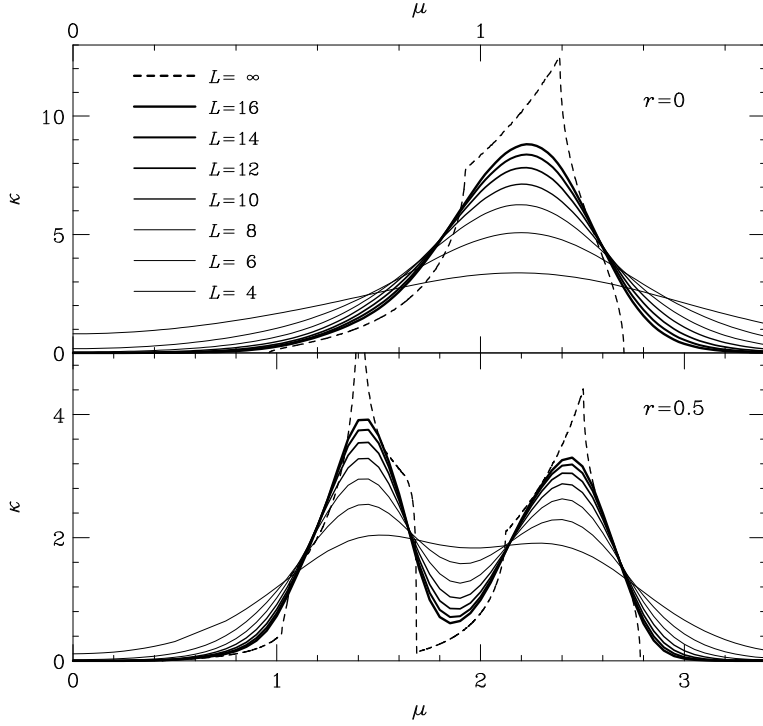


Figure 7: Same as Fig. 6 for  $r = 0$  and  $r = 0.5$ .

can be straightforwardly generalized to interacting systems, but its equivalence with the Kohn's method is just an ansatz. Nevertheless the agreement is excellent, as we will show.

By analogy with continuum electrodynamics, we want to study the electric current induced in the system by an external weak uniform electric field in the 1 direction. The conductivity (in Fourier Space), will be the proportionality constant between the electrical current and the external field.

There are some subtleties that need to be considered when putting an external electric field on the lattice. We take the gauge-field configuration ( $t = x_0$ )

$$U_{x,0} = e^{i E_t x_1}, \quad U_{x,i} = 1, \quad (79)$$

$$E_t = \frac{2\pi}{L_1} n_t, \quad n_t \in \left\{ -\frac{L_1}{2}, -\frac{L_1}{2} + 1, \dots, \frac{L_1}{2} - 1, \frac{L_1}{2} \right\}. \quad (80)$$

Notice that the quantization of the electric-field is due to the spatial boundary conditions (in the following, we shall only indicate the non-vanishing  $n'_i$ 's). To preserve the translational symmetry, the displaced gauge field

$$U_{x,0} = e^{i E_t (x_1 - \xi)}, \quad \xi \text{ integer}, \quad (81)$$

should be a gauge-transform of the one in Eq. (79). Since the needed gauge transformation is analogous to Eq. (54), it is easy to check that the condition that allows this transformation is the trivialness of the Polyakov loop:

$$\prod_{t=0}^{L_0-1} U_{(t,x),0} = 1 \quad \text{or} \quad \sum_{t=0}^{L_0-1} E_t = 2\pi n, \quad (82)$$

with  $n$  integer. This condition also allows to transform the gauge field to the Coulomb gauge  $A_0 = 0$ . If condition (82) is violated, the translational invariance is lost and the electric current is no longer spatially homogeneous even on a homogeneous electric-field. However, with the correct field choice (82), we get a homogeneous electrical current aligned with the external electrical field, and imaginary as anticipated in

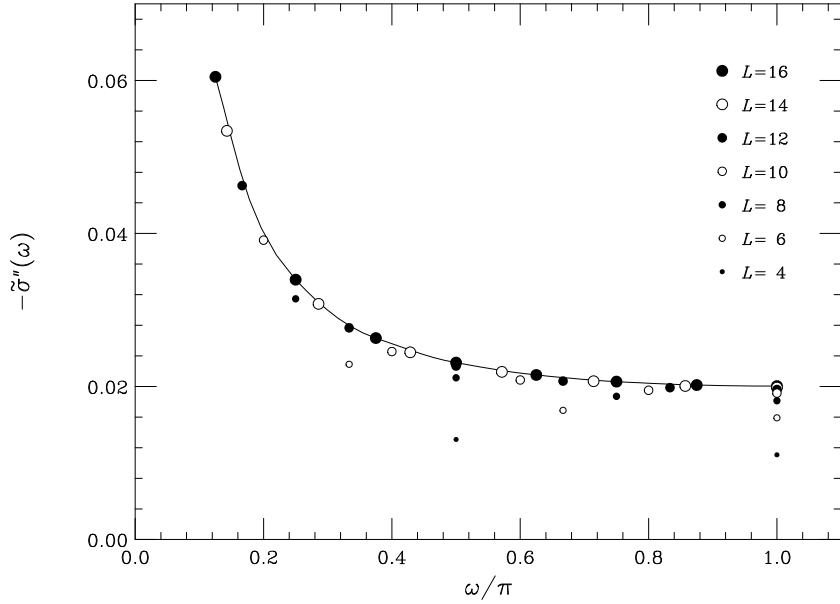


Figure 8: The imaginary part of the conductivity  $\tilde{\sigma}(\omega)$  of a system of free Wilson fermions at  $r = 1$ ,  $m = 1/2$  and  $\mu = 1$ .

Eq. (29). In order to directly compare with the results obtained with Eq. (57), let us define

$$j(t) = i\langle j_{x,1} \rangle \quad (83)$$

If we want to stay within linear-response theory, we have to postulate a linear relation between the Fourier transform of the electrical current  $j(t)$  and the external electrical field  $E_t$ :

$$\hat{j}(\omega) = \sigma(\omega) \hat{E}(\omega). \quad (84)$$

Notice that both  $j(t)$  and  $E_t$  being real,  $\sigma(-\omega) = \sigma^*(\omega)$ . However, the results can be more cleanly cast in terms of a modified Fourier transform for the electrical field:

$$\tilde{E}(\omega) = \frac{1}{\sqrt{L_0}} \sum_{t=0}^{L_0-1} E_t e^{-i\omega(t+1/2)}. \quad (85)$$

The rationale for this is that the electrical field  $E_t$  on the lattice lives mid-way between sites at times  $t$  and  $t+1$ . The modified conductivity  $\tilde{\sigma}(\omega) = \hat{j}(\omega)/\tilde{E}(\omega)$  is related with the previous one by

$$\tilde{\sigma}(\omega) = \sigma(\omega) e^{i\omega/2}. \quad (86)$$

The nice feature of  $\tilde{\sigma}(\omega)$  is that it turns out to be purely imaginary.

In Fig. 8 we plot the imaginary part of  $\tilde{\sigma}(\omega)$  as obtained from a field with  $n_0 = 1$  and  $n_1 = -1$ , in a system of Wilson fermions with  $m = 1/2$ ,  $r = 1$  and  $\mu = 1$ , that is within the band energy-range and therefore with a non-vanishing Fermi surface (see Fig. 3). We see that for large frequencies the thermodynamic limit is reached in rather small lattices. However, at the minimal reachable frequency ( $2\pi/L_0$ ) the conductivity is rapidly growing suggesting a singularity at zero frequency. In fact, for a (classical) system of free particles of density  $n$  we expect that  $\sigma(\omega)$  will behave as

$$\sigma_{\text{free, classical}} \sim -i \frac{e^2 n}{m \omega}. \quad (87)$$

Notice that if  $\sigma(\omega)$  has a pole at  $\omega = 0$  with a purely imaginary residue the same will hold true for  $\tilde{\sigma}(\omega)$ , and both residues will be equal. Although the *Euclidean* conductivity  $\tilde{\sigma}(\omega)$  do not match the real-time

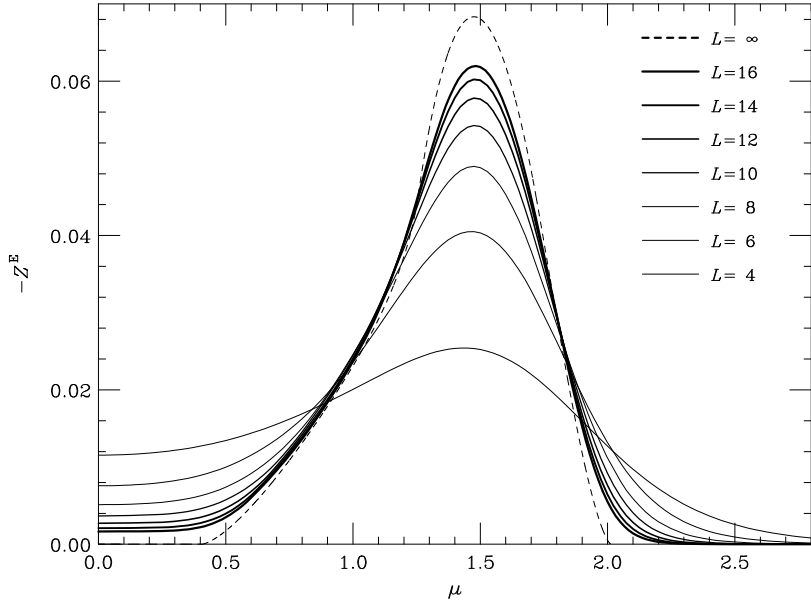


Figure 9: The finite-size residue  $Z^E$ , for a system of fermions with  $m = 1/2$ ,  $r = 1$  at  $\omega = \omega_{\min} = 2\pi/L_0$ . The infinite volume limit has been obtained with the Kohn's method Eq. (57).

one (being imaginary, it cannot fulfill the Kramers-Kronning relations), one can formally expect the residues to coincide in the passage from  $\omega$  to  $i\omega$ . This suggest to define the following quantity which will be the basic object of our study:

$$Z^E = \frac{1}{i}\omega^{\min}\tilde{\sigma}(\omega^{\min}), \quad \omega^{\min} = \frac{2\pi}{L_0}. \quad (88)$$

In the  $L_i, L_0 \rightarrow \infty$  limit,  $Z^E$  tend to the residue of the pole. In order to measure this, we have considered the smallest of possible external disturbances:  $\{n_0 = 1, n_{L_0/2} = -1\}$ .

Our results can be found in Figs. 9, and 10. We see that the *Euclidean* residue follows quite closely Kohn's result, which in fact can be considered as the infinite volume limit for our calculation. Moreover, the physical picture presented during the band structure discussion is nicely confirmed: when the band is full, the system gets rather inert, while when the band is empty, it can be excited by the external field creating a hole in the lower band. Since the smallest possible excitation has frequency  $2\pi/L_0$ , to be compared with a gap  $2m$ , it is rather reasonable that at  $\mu = 0$ , the larger is the space-time lattice, the smaller is the system response. In fact, notice that in Figs. (9,10) when  $\mu$  is below the lower band limit, the curves get horizontal: in this range of  $\mu$  the system can be only excited by crossing the gap between the inner and the conduction band. And the gap is, of course,  $\mu$  independent in a non-interacting system.

We remark that our results have been found within the linear response approximation. We can control this approximation in several ways. One is to study the Fourier transform of the current, for frequencies at which the Fourier transform of the external-field vanishes. In Fig. 11 we show the zero-mode of the electrical current for the electrical-field  $\{n_0 = 1, n_1 = -1\}$ . We see that this non-linear effect tends to zero with growing lattice-size, which is quite reasonable since the minimum possible electric field is  $2\pi/L_1$ . The non-linear corrections are oscillating, but modulated by a rapidly decaying function. A different test can be done, by considering the residue obtained with an stronger electric-field  $\{n_0 = 2, n_{L_0/2} = -2\}$  (see the circles in Fig. 10). Roughly speaking, for the largest lattice the non linear effects are of the same order as the distance to the thermodynamic limit. A further check can be done by comparing the residue obtained from the data in Fig. 8 with the one in Fig. 9: in the  $L = 14$  lattice, the differences are at the 0.3% level, while in the  $L = 6$  lattice the differences are at the 1.6% level. Therefore, we believe that non-linear effects are under control for the not too small fields that we can deal with.

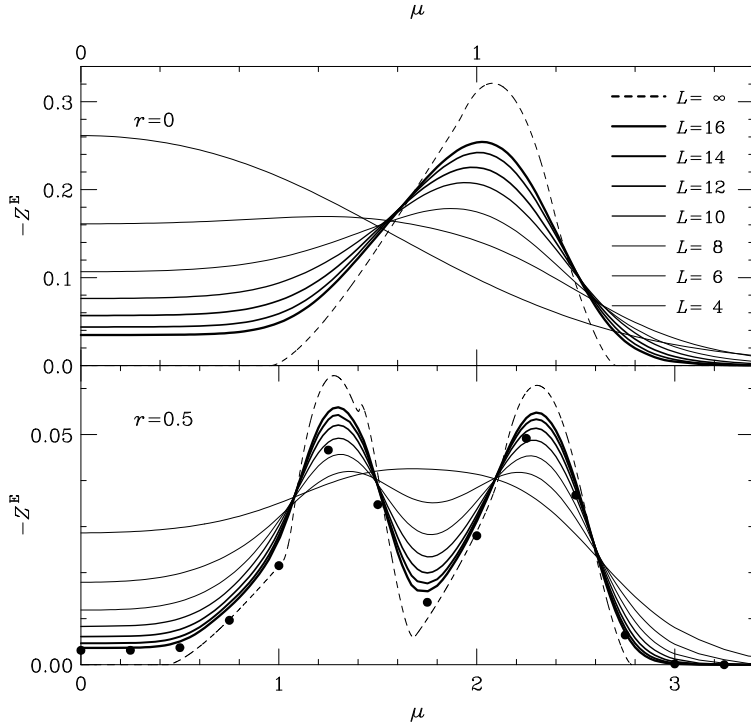


Figure 10: Same as Fig. 9 but for  $r = 0$  and  $r = 0.5$ . The dots, in the  $r = 0.5$  case, have been obtained in an  $L = 16$  lattice, with an electrical field twice larger.

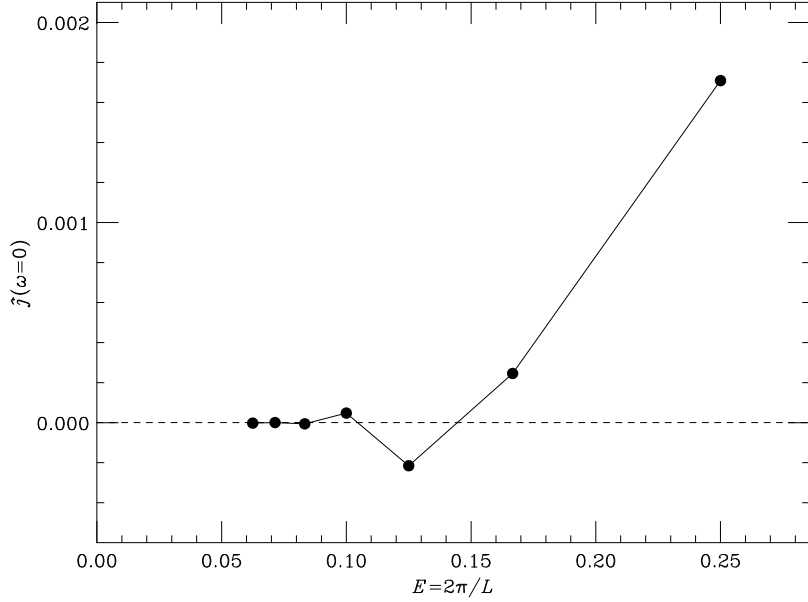


Figure 11: The Fourier transform at zero frequency of the electrical current as a function of the inverse lattice size.

## 7 Conclusions

We have studied a system of *free* Wilson fermions at finite density. The model is studied both in a Hamiltonian and in a path-integral formalism, and it is shown that the model presents a band structure.

The path-integral formalism can be easily generalized to consider interactions with an external electro-magnetic field, or even self-interactions. The Hamiltonian theory is recovered after performing a simple continuum-time extrapolation.

We have computed the density of states both analytically and numerically in a finite lattice, obtaining a nice thermodynamic limit convergence. In addition, we have analytically computed the residue of the zero frequency pole of the conductivity, using a method proposed by Kohn. The results has been contrasted with a numerical computation based on the linear response to an external electric field in Euclidean time, with an excellent agreement.

In contrast with the analytical calculation which can only be done for a non interacting system (or, at most, in an homogeneous external gauge field), the numerical calculations are easily generalizable to more complex models, as fermions self-coupled with quartic interactions or via a dynamic bosonic field.

After the time continuum limit is performed, our model has two remaining free parameters:  $r_s$  and  $m$  that can be chosen depending on the particular physical system of interest. The mass  $m$  fixed the energy distance with the lower band, while the Wilson parameter  $r_s$  allows to reshape the dispersion relation.

The next step will be the application of this methods to systems of interest in Condensed Matter Physics. Specifically, a study of a system of fermions coupled to a dynamic bosonic field is in project.

An open, very interesting question is the possibility of extracting the full real-time electrical conductivity function from its *Euclidean* counterpart. We have shown that the residue of the zero-frequency pole can indeed be obtained.

## 8 Acknowledgements

This work was triggered during a discussion with F. Guinea to whom we are indebted for many suggestions, discussions and bibliographical help. The numerical calculations have being carried-out in the RTNN machines at the universities of Zaragoza and Complutense de Madrid. This work has been partially supported by CICYT, contracts AEN97-1680,1693,1708.

## References

- [1] J.G. Bednorz, K.A. Müller, Z. Phys. **C64**(1986)188.
- [2] *Colossal Magnetoresistance, Charge Ordering and Related Properties of Manganese Oxides*. World Scientific 1998. Editors, C.N.R. Rao and B. Raveau.
- [3] *Strongly Correlated Magnetic and Superconducting Systems*, Lecture Notes in Physics 478, Springer 1997 . Editors, G. Sierra and M.A. Martín-Delgado.
- [4] C. Zener, Phys. Rev. **82**(1951)403; P.W. Anderson, H. Hasegawa, Phys. Rev. **100**(1955)675; P.G. de Gennes, Phys. Rev. **118**(1960)141.
- [5] J.L. Alonso, Ph. Boucaud, V. Martín-Mayor, and A.J. van der Sijs, Europhys. Lett. **42**(1998)541.
- [6] K.G. Wilson, Phys. Rev. **D14**(1974)2455.
- [7] *Quantum Fields on the Computer*, World Scientific, Vol.11 1992. Edited by Michael Creutz
- [8] F. Karsch, J.B. Kogut, and H.W. Wyld, Nucl. Phys. **B280**[FS18](1987)289; S.J. Hands, A. Kocić and J.B. Kogut, Nucl. Phys. **B390**(1993)355; S.J. Hands, S. Kim and J.B. Kogut, Nucl. Phys. **B442**(1995)364; I. Barbour, S. Hands, J.B. Kogut, M-P. Lombardo, S. Morrison, hep-lat/9902033.
- [9] *QCD at Finite Barion Density*, Nucl. Phys. **A642**(1998) Proc. Supp. Nos. 1-2, Edited by F. Karsch and M-P. Lombardo.
- [10] K.G. Wilson. *Quarks and Strings on the Lattice*, in New Phenomena in subnuclear Physics. Editor A. Zichichi. Plenum Press, New York 1977.
- [11] I. Montvay and G. Münster, *Quantum Fields on a Lattice*. Cambridge Univ. Press. 1994.

- [12] W. Kohn, Phys. Rev. **133**(1964)A171.
- [13] J.B. Kogut, Rev. Mod. Phys. **51**(1979)659.
- [14] P. Hasenfratz, F. Karsch, Phys. Lett. **B125**(1983)308.
- [15] J.B. Kogut, H. Matsuoka, M. Stone, H.W. Wyld, S. Shenker, J. Shigemitsum D.K. Sinclair, Nucl. Phys. **B225**[FS9](1983)93.
- [16] I. Bender, H.J. Rothe, I.O. Stomatescu, W. Wetzel, Z. Phys. **C58**(1993)333.
- [17] R.V. Gavai, Phys. Rev. **D32**(1985)519.
- [18] N.W. Ashcroft and N.D. Mermin, *Solid State Physics*, Saunders College Publishing, 1976.